Elemental Carbon Chain Bridging Two Iron Centers: Syntheses and Spectroscopic Properties of Donor−Acceptor [Fe]−C_4−[Fe] Complexes Isolated in Two Different Oxidation States. X-ray Crystal Structure of [Cp*(dppe)Fe−C_4−$Fe(CO)_2$Cp*]

Françoise Coat,[†] Marie-Andrée Guillevic,[†] Loic Toupet,[‡] Frédéric Paul,[†] and Claude Lapinte*,[†]

UMR CNRS 6509 Organométalliques et Catalyse and UMR CNRS 6626 Groupe Matière Condensée et Matériaux, Université de Rennes I, Campus de Beaulieu, 35042 Rennes Cedex, France

Received August 18, 1997[⊗]

The complexes $Fe(\eta^5\text{-}C_5R_5)(CO)_2(C{\equiv}CC{\equiv}CSiMe_3)$ (R = Ph, **2a**; R = Me, **2b**) were obtained from the reaction of $(\eta^5\text{-}C_5Ph_5)Fe(CO)_2Br$ (**1a**) or (Cp*)$Fe(CO)_2I$ (Cp* = $\eta^5\text{-}C_5Me_5$, **1b**) with $Me_3SiC{\equiv}CC{\equiv}CLi$ (1.05 equiv) in THF at −80 °C (70−75%). The butadiynyl complex $(\eta^5\text{-}C_5Me_5)Fe(dppe)(C{\equiv}CC{\equiv}CSiMe_3)$ (**2c**) was prepared upon photolysis of **2b** in a toluene/acetonitrile mixture (95/5 v/v) in the presence of dppe (1,2-bis(diphenylphosphino)ethane) (85%). Treatment of complexes **2a**,**2b** with 1.1 equiv of potassium fluoride in a 50/50 CH_3-OH/THF mixture at 20 °C afforded the terminal butadiyne complex $(\eta^5\text{-}C_5R_5)Fe(CO)_2$-$(C{\equiv}CC{\equiv}CH)$ (R = Ph, **3a**; R = Me, **3b**), isolated in 85 and 95% yields respectively. Complex **3c** was obtained by reaction of **2c** with 0.2 equiv of $Bu^n{}_4NF$ in THF (95%). The mononuclear complexes **2a**−**c** and **3a**−**c** were characterized by cyclic voltammetry and IR, ^1H, ^{13}C, and ^{31}P NMR, and Mössbauer spectroscopy. The binuclear complexes **5a,b** were obtained (59−69%) in a one-step procedure by treatment of $(\eta^5\text{-}C_5R_5)Fe(CO)_2(C{\equiv}CC{\equiv}CH)$ (**3a,b**) with 1 equiv of Cp*Fe(dppe)Cl (**4**) in the presence of KPF_6 and $KOBu^t$ in methanol. The lower IR frequencies of the carbonyl groups in **5a,b** relative to the isolated acceptor group in **2a,b** and **3a,b** are indicative of the electronic communication between the metal centers through the $-C_4-$ spacer. In the complexes **5a,b**, the polarization of the spacer was shown by the ^{13}C NMR chemical shifts of the carbon of the $-C_4-$ chain. The Mössbauer spectrum of **5b** establishes that the electron density at the two iron atoms is quite different. The structure of **5b** has been determined by X-ray diffraction. Cyclic voltammograms of complexes **5a,b** from −0.8 to −1.4 V/SCE displayed one fully reversible wave and a second one almost reversible, showing that the binuclear systems undergo two successive one-electron oxidations at the electrode. Comparison of both redox potentials and current ratio with those of the corresponding monomers **2a**−**c** demonstrates that a strong electronic communication between the metal centers takes place across the all-carbon bridge. Treatment of the neutral complexes with 1 equiv of ferrocenium allowed isolation of the salts **[5a,b][PF_6]** in 85−90% yield. Mössbauer spectroscopy showed that both salts were trapped Fe(II)-Fe(III) mixed-valence compounds. The **g** tensors and couplings with the ^{31}P nuclei are very close for both Fe(III) low-spin radicals. Intense absorption bands were observed at 810 and 829 nm for **[5a][PF_6]** and **[5b][PF_6]**, respectively. A second absorption band was observed in the near-infrared for **[5b][PF_6]** (1600 nm) and ascribed to an ICT band. It allowed determination of the electronic coupling between the electron-poor and the electron-rich iron centers through the all-carbon spacer (V_{ab} = 0.021 eV).

Elemental carbon chains constitute the simplest molecular wires that one can imagine.[1−3] In these linear and rigid connectors the carbon atoms are sp-hybridized with alternate single and triple bonds between the carbon atoms. Among those, the carbon chains with redox-active terminal end groups are particularly interesting, since a change in the oxidation state of one terminal group is conveyed through the carbon wire and modifies the properties of the other end group. Thus, the carbon spacer operates as a molecular wire permitting electrons to flow between the redox centers. As a consequence of this electronic communication, two chemically identical redox-active end groups show two different redox potentials. The separation between them can be determined by voltammetry and constitutes a measure of the electron conduction in this basic electronic circuit. The intensity of this effect depends upon both of the redox centers and the spacer. It is significantly stronger for complexes having the general formula $L_nM-C_x-ML_n$[4−9] than for those with other

[†] UMR CNRS 6509 Organométalliques et Catalyse.
[‡] UMR CNRS 6626 Groupe Matière Condensée et Matériaux.
[⊗] Abstract published in *Advance ACS Abstracts*, December 1, 1997.

(1) Rice, M. J.; Bishop, A. R.; Campbell, D. K. *Phys. Rev. Lett.* **1983**, *51*, 2136.
(2) Ward, M. D. *Chem. Ind. (London)* **1996**, 568−573.
(3) Harriman, A.; Ziessel, R. *Chem. Commun.* **1996**, 1707−1716.

S0276-7333(97)00730-9 CCC: $14.00

Scheme 1

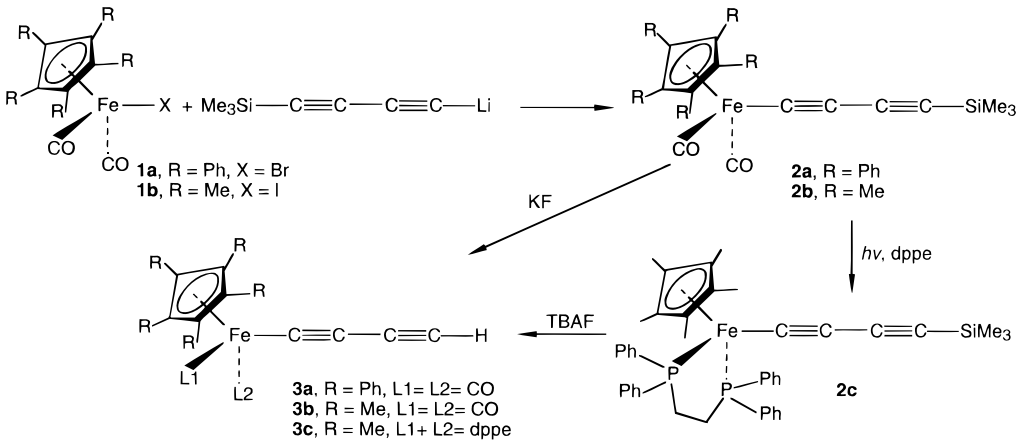

types of unsaturated bridges.[10−14] In these molecular devices, the redox potentials of the metal centers are quite different from the potential of the mononuclear isolated compounds. Moreover, the electrochemical reversibility of the redox process can also be strongly affected by electron delocalization between the metal and the all-carbon bridge. Up to now, this effect had never been evidenced in donor−acceptor organometallic compounds with a large extent of delocalization of the valence electrons.[15]

We have previously reported the synthesis and the characteristic features of the three-redox-state family of compounds $[Cp^*(dppe)FeC{\equiv}CC{\equiv}CFe(dppe)Cp^*]^{n+}$-$[PF_6^-]_n$ ($n = 0-2$).[5,6] This study, together with important and complementary results obtained in a similar rhenium series,[7−9] has both revealed the very special coupling properties of the $-C_x-$ ligand in dinuclear complexes and shown the versatility of the electronic structure of the coordinated carbon chains. More recently, the particular properties of the $[M]-C_4-[M]$ assembly were illustrated with diruthenium complexes.[16] In these systems, the carbon bridge was connected to two identical redox-active termini and electron transfer occurred in a symmetrical way.

In contrast, a linear spacer bearing an electron acceptor on one end and an electron donor on the other should display preferential one-way electron transfer and act as a rectifying component.[17] Such molecular devices can be seen as polarized molecular wires. If one of the terminal groups is redox-active and stable at least under two different oxidation states, these systems can also constitute models for electro-switchable molecular current rectifiers or NLO-active materials. In this respect, we were interested in the properties of the polarized $D-C_4-A$ organometallic assembly in which the donor (D) and the acceptor (A) termini are organoiron building blocks with quite different electronic densities. The model that we designed in this work comprises the electron-rich redox-active Cp*Fe(dppe) center as the donor end, and the electron-withdrawing $(C_5R_5)Fe(CO)_2$ (R = Ph, Me) units, which are not redox-active in mononuclear complexes, on the other side. Thus, we will now report (i) the synthesis of the $-C_4-$ bridged bimetallic complexes $[(C_5Me_5)(dppe)Fe(C{\equiv}CC{\equiv}C)Fe(CO)_2(C_5R_5)]^{n+}[PF_6^-]_n$ (R = Ph, $n = 0$, **5a**; R = Ph, $n = 1$, **5a[PF$_6$]**; R = Me; $n = 0$, **5b**; R = Me, $n = 1$, **5b[PF$_6$]**), (ii) their full spectroscopic characterizations, including an X-ray crystal structure of the compound **5b**, (iii) a cyclic voltammetry study, showing the strong metal−metal electronic communication both in terms of redox potentials and chemical reversibility, (iv) a spectroscopic study of the charge transfer and the electronic coupling between the two redox centers in the mixed valence complexes. The spectroscopic and redox properties of the related mononuclear complexes are given as well in a preliminary study.

Results and Discussion

1. Synthesis and Characterization of the Butadiynyl Complexes $(C_5R_5)Fe(L)_2(C{\equiv}CC{\equiv}CR')$. Following a known procedure,[18] the complexes $Fe(\eta^5-C_5R_5)(CO)_2(C{\equiv}CC{\equiv}CSiMe_3)$ (R = Ph, **2a**; R = Me, **2b**) were obtained from the reaction of the corresponding iron halide $(\eta^5-C_5Ph_5)Fe(CO)_2Br$ (**1a**)[19,20] or $(\eta^5-C_5Me_5)Fe(CO)_2I$ (**1b**)[21] with $Me_3SiC{\equiv}CC{\equiv}CLi$[22] (1.05 equiv) in THF at −80 °C. The (trimethylsilyl)butadiynyliron complexes **2a,b** were isolated after crystallization as yellow powders in 70 - 75% yield (Scheme 1).

The butadiynyl complex $(\eta^5-C_5Me_5)Fe(dppe)(C{\equiv}CC{\equiv}CSiMe_3)$ was prepared upon photolysis of **2b** in toluene. After 4 h of irradiation, the dark brown solution was evaporated to dryness, and crystallization

(4) Coat, F.; Lapinte, C. *Organometallics* **1996**, *15*, 477−480.
(5) Le Narvor, N.; Lapinte, C. *J. Chem. Soc., Chem. Commun.* **1993**, 357−359.
(6) Le Narvor, N.; Toupet, L.; Lapinte, C. *J. Am. Chem. Soc.* **1995**, *117*, 7129−7138.
(7) Brady, M.; Weng, W.; Gladysz, J. A. *J. Chem. Soc., Chem. Commun.* **1994**, 2655−2656.
(8) Seyler, J.; Weng, W.; Zhou, Y.; Gladysz, J. A. *Organometallics* **1993**, *12*, 3802−3804.
(9) Brady, M.; Weng, W.; Zhou, Y.; Seyler, J. W.; Amoroso, A. J.; Arif, A. M.; Böhme, M.; Frenking, G.; Gladysz, J. A. *J. Am. Chem. Soc.* **1997**, *119*, 775−788.
(10) Ward, M. D. *Chem. Soc. Rev.* **1995**, 121.
(11) Creutz, C. *Prog. Inorg. Chem.* **1983**, *30*, 1−73.
(12) Crutchly, R. J. *Adv. Inorg. Chem.* **1994**, *41*, 273.
(13) Ribou, A. C.; Launay, J. P.; Sachtleben, M. L.; Li, H.; Spangler, C. W. *Inorg. Chem.* **1996**, *35*, 3735−3740.
(14) Bunz, U. H. F. *Angew. Chem., Int. Ed. Engl.* **1996**, *35*, 969−971.
(15) Sato, M.; Shintate, H.; Kawata, Y.; Sekino, M. *Organometallics* **1994**, *13*, 1956−1962.
(16) Bruce, M. I.; Denisovich, L. I.; Low, P. J.; Peregudova, S. M.; Ustynyuk, N. A. *Mendeleev Commun.* **1996**, 200−201.
(17) Astruc, D. *Electron Transfer and Radical Processes in Transition-Metal Chemistry*; VCH: New York, 1995.
(18) Wong, A.; Kang, P. C. W.; Tagge, C. D.; Leon, D. R. *Organometallics* **1990**, *9*, 1992−1994.
(19) Vey, S. M.; Pauson, P. L. *J. Chem. Soc.* **1965**, 4312.
(20) Brégaint, P.; Hamon, J.-R.; Lapinte, C. *J. Organomet. Chem.* **1990**, *398*, C25−C28.
(21) Akita, M.; Terada, M.; Oyama, S.; Moro-Oka, Y. *Organometallics* **1990**, *9*, 816−825.
(22) Holmes, A. B.; Jennings-White, C. L. D.; Schulthess, A. H.; Akinde, B.; Walton, D. R. M. *J. Chem. Soc., Chem. Commun.* **1979**, 840−842.

Table 1. IR Spectral Data for the Organoiron Butadiynyl Complexes (KBr/Nujol, cm^{-1})

compd	end groups		ν_{CO}	$\nu_{C\equiv C}$
2a	$(C_5Ph_5)Fe(CO)_2$	$SiMe_3$	2024, 1984	2185, 2129
2b	$(C_5Me_5)Fe(CO)_2$	$SiMe_3$	2031, 2017, 1970	2171, 2120
2c	$(C_5Me_5)Fe(dppe)$	$SiMe_3$		2165, 2090, 1980
3a	$(C_5Ph_5)Fe(CO)_2$	H	2033, 1988	2141
3b	$(C_5Me_5)Fe(CO)_2$	H	2020, 1964	2142
3c	$(C_5Me_5)Fe(dppe)$	H		2099, 1958
5a	$(C_5Me_5)Fe(dppe)$	$(C_5Ph_5)Fe(CO)_2$	2022, 1976	2102
5b	$(C_5Me_5)Fe(dppe)$	$(C_5Me_5)Fe(CO)_2$	2013, 1952	2109
5a$^+$	$(C_5Me_5)Fe(dppe)$	$(C_5Ph_5)Fe(CO)_2$	2037, 1993	*a*
5b$^+$	$(C_5Me_5)Fe(dppe)$	$(C_5Me_5)Fe(CO)_2$	2032, 1989	1967, 1906

[a] The $\nu_{C\equiv C}$ bond stretching is obscured by the carbonyl vibrations.

Table 2. ^{13}C NMR (20 °C, C_6D_6) Chemical Shifts (ppm) for the C_4 Chain[a]

compd	end groups		C_α	C_β	C_γ	C_δ
2a	$(C_5Ph_5)Fe(CO)_2$	$SiMe_3$	99.8	99.4	92.6	71.7
2b	$(C_5Me_5)Fe(CO)_2$	$SiMe_3$	106.3	96.5	94.7	69.5
2c	$(C_5Me_5)Fe(dppe)$	$SiMe_3$	142.2	102.3	96.2	69.7
3a	$(C_5Ph_5)Fe(CO)_2$	H	94.1	99.7	72.8	55.9
3b	$(C_5Me_5)Fe(CO)_2$	H	102.9	95.0	73.4	54.1
3c	$(C_5Me_5)Fe(dppe)$	H	136.6	100.7	75.1	50.5
5a	$(C_5Me_5)Fe(dppe)$	$(C_5Ph_5)Fe(CO)_2$	114.4	108.7	108.3	86.9
5b	$(C_5Me_5)Fe(dppe)$	$(C_5Me_5)Fe(CO)_2$	107.4	108.5	102.4	68.3

[a] In the binuclear compounds the carbon atoms are named $C_{\alpha-\delta}$ starting from the more electron-rich iron center Cp*Fe(dppe).

of the solid residue from CH_2Cl_2/pentane afforded **2c** in 40% yield. We noted a strong dependency of the yield of the reaction upon concentration of the starting materials, which could be due to a competitive coordination of the terminal acetylenic function of the butadiynyl chain. Addition of 5% (v/v) of CH_3CN in toluene greatly improved the procedure. Indeed, after irradiation, the solution became red-orange this time, and washing with cold ether provided 70% of **2c**. The acetonitrile ligand is believed to temporarily replace the photodisplaced carbonyl groups before the diphosphine coordinates to the metal. This contrasts with the photochemical displacement of the carbonyl ligands by the dppm in the related ethynyl complex $(C_5H_5)Fe(dppm)(C\equiv CR)$, where assistance of a coordinating solvent is not required.[23]

Treatment of complexes **2a,b** with 1.1 equiv of potassium fluoride in a 50/50 CH_3OH/THF mixture at room temperature gave the respective terminal butadiyne complexes $Fe(\eta^5\text{-}C_5Re_5)Fe(CO)_2(C\equiv CC\equiv CH)$ (**3a,b**), isolated as brown and yellow solids in 85 and 95% yields respectively. Surprisingly, **2c** does not react under the above conditions even under reflux. However, we found that catalytic cleavage of the trimethylsilyl group in **3c** is readily effected in pure THF using 0.2 equiv of Bu^n_4NF. This route, which provided **3c** as an orange-red solid in 95% yield, was previously used for the desilylation of similar organometallic compounds.[18,24]

The mononuclear analytically pure complexes **2a**−**c** and **3a**−**c** were characterized by cyclic voltammetry and IR, ^1H, ^{13}C, and ^{31}P NMR, and Mössbauer spectroscopy. IR spectra featured $\nu_{C\equiv C}$ and ν_{CO} bands (Table 1). It is noteworthy that IR spectra of the complexes **2a**−**c** which bear a trimethylsilyl group at one end of the butadiynyl ligand exhibit one more C≡C band stretching than the corresponding complexes **3a**−**c**. Three vibrational modes are observed for the carbonyl ligands of **2b** and for the $\nu_{C\equiv C}$ bands of **2c**. These unusual observations could possibly result from the coupling of one of the expected normal modes with another oscillator.[25,26] A decrease of both the $\nu_{C\equiv C}$ and ν_{CO} frequencies with increasing electronic density at the iron center is observed for the series of compounds **2** and **3**. These wavenumbers are clearly suggestive of an increase in the retrodonation from the metal center in π^*_{CO} or $\pi^*_{C\equiv C}$. If this interpretation fits very well with current knowledge for the carbonyl groups, it is rather unexpected for the ethynyl and butadiynyl ligands. Indeed, it has been reported that the filled/filled interactions between the occupied metal dπ orbitals and π orbitals of the $-C_2-$ or $-C_4-$ fragment was the dominant interaction taking place in the $CpFe(CO)_2$ series, retrodonation occurring only to a negligible extent.[27] However, in the more electron rich Cp*Fe(dppe) series the present results, including the X-ray analysis of complex **5b** (*vide infra*), together with other IR data obtained on $Cp^*Fe(dppe)(C\equiv CC_6H_4X)$ complexes[28] could indicate that a weak retrodonation in the π^* orbitals takes place.

The ^{13}C NMR resonances of the $-C_4-$ chain were easily observed, and the chemical shifts of the carbon atoms proved to be sensitive to the nature of the terminal groups (Table 2). The carbon resonances of the butadiynyl ligand can unequivocally be assigned on the basis of the J_{CH} and J_{CP} coupling constants in the case of the complex **3c**. Indeed, the ^{13}C resonances of the $-C_4H$ fragment are located in the spectrum at δ 50.5 (C_δ, d, $^1J_{CH} = 248$ Hz), 75.1 (C_γ, dt, $^2J_{CH} = 50$ Hz, $^4J_{PC} = 3$ Hz), 100.7 (C_β, d, $^3J_{CH} = 5$ Hz) and 136.6 (C_α, t, $^2J_{PC} = 38$ Hz). Comparison of the J_{CH} and J_{CP} coupling constants establishes that $^4J_{CP}$ is larger than $^3J_{CP}$, whereas the $^4J_{CH}$ coupling constant was too small to be observed. For **3a,b** similar attributions were made. An upfield resonance was attributed to C_β (δ 99.7, $^3J_{CH} = 5.8$ Hz) relative to C_α (δ 94.1, s) in compound **3a**. Accordingly, in the case of the trimethylsilyl homologue

(23) Gamasa, M. P.; Gimeno, J.; Lastra, E.; Lanfranchi, M.; Tiripicchio, A. *J. Organomet. Chem.* **1991**, *405*, 333−345.
(24) Sun, Y.; Taylor, N. J.; Carty, A. J. *Organometallics* **1992**, *11*, 4293−4300.
(25) Wojtkowiak, B. *Ann. Chim.* **1964**, *9*, 5−24.
(26) Fontaine, M.; Chauvelier, J.; Barchewitz, P. *Bull. Soc. Chim. Fr.* **1962**, *359*, 2145−2150.
(27) Lichtenberger, D. L.; Renshaw, S. K.; Wong, A.; Tagge, C. D. *Organometallics* **1993**, *12*, 3522−3526.
(28) Denis, R.; Weyland, T.; Paul, F.; Lapinte, C. *J. Organomet. Chem.*, in press.

Table 3. Electrochemical Data for Compounds 2−5[a]

compd	ΔE_p	E_0	i^c/i^a	ΔE_0
2a		−0.97	NR	
2b		+1.15	NR	
2c	0.09	+0.00	1	
3a		−0.87	NR	
3b		−1.30	NR	
3c	0.09	0.00	0.48	
5a	0.06	−0.28	1	1.21
	0.07	+0.93	0.8	
5b	0.07	−0.36	1	1.10
	0.07	+0.74	0.9	

[a] All E and ΔE values in V vs SCE. NR = nonreversible. Conditions: CH_2Cl_2 solvent; 0.1 M $[nBu_4N][PF_6]$ supporting electrolyte; 20 °C; Pt electrode; sweep rate 0.100 V s−1. The ferrocene−ferrocenium couple (0.460 V vs SCE) was used as an internal reference for the potential measurements.

2a, an upfield resonance was attributed as well to C_β (δ 99.7) relative to C_α (δ 94.4), since those carbon resonances were observed at a very close position. A more intuitive assignment was proposed for the other compounds. Thus, substitution of the trimethylsilyl group with a hydrogen atom or the substitution of an ancillary ligand at the iron center results in variations of the chemical shifts of the carbon atoms of the chain. This can be taken as an indication of good communication between the end groups and the butadiyne π-system.

The cyclic voltammograms (CV) of the butadiyne complexes $(C_5R_5)Fe(CO)_2(C{\equiv}CC{\equiv}C\text{-}SiMe_3$ (**2a,b**) from −1.5 to +1.5 V display one wave at a platinum electrode (dichloromethane, 0.1 M tetrabutylammonium hexafluorophosphate, 0.100 V s^{-1}, 20 °C, Table 3). The very different electrochemical behaviors observed for these two complexes illustrate the opposite electronic effects of the C_5Ph_5 and C_5Me_5 cyclic ligands, which stabilize respectively the low and high oxidation states. Thus, the very electron-poor complex $(C_5Ph_5)Fe(CO)_2$-$(C{\equiv}CC{\equiv}CSiMe_3)$ (**2a**) shows an irreversible reduction wave at −0.99 V corresponding to the Fe(II)/Fe(I) redox system. The CV of the complex $(C_5Me_5)Fe(CO)_2$-$(C{\equiv}CC{\equiv}CSiMe_3)$ (**2b**) exhibits an irreversible oxidation wave at +1.18 V attributed to the Fe(II)/Fe(III) redox couple. Replacement of the two CO ligands by dppe stabilizes the 17-electron iron(III), and a fully reversible oxidation wave is observed for the complex $(C_5Me_5)Fe$-$(CO)_2(C{\equiv}CC{\equiv}CSiMe_3)$ (**2c**) with an i_p^a/i_p^c current ratio of unity (E_0 = −0.01 V vs SCE). As in the previous ethynyl series, the presence of a bulky terminal end group is still required to stabilize the iron(III) butadiynyl radical cation, since the compound **3c** shows only a partially reversible oxidation process (Table 3).[6,29]

The Mössbauer spectral parameters of a recrystallized sample of the mononuclear complexes **2b,c** and **3c** recorded at zero field (80 K) are typical of pure iron(II) centers with a quadrupole splitting weakly dependent on the ligands coordinated to the metal (Table 4). A significant increase of the isomeric shift from 0.017 to 0.245 mm/s associated with an increase of the electron density at the iron center. The Mössbauer parameters of the iron(II) and iron(III) sites in the Cp*Fe(dppe)R series are usually weakly dependent on the temperature.[30] This general trend is confirmed for the butadiynyl derivatives in the case of complex **2c**.

Scheme 2

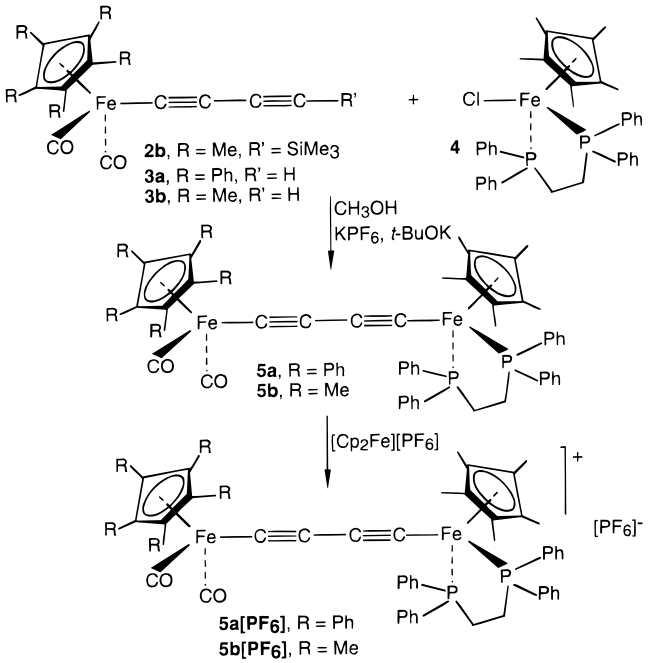

2. Synthesis and characterization of the binuclear μ-butadiyndiyl complexes (C_5Me_5)(dppe)-Fe(C≡CC≡C)Fe(CO)$_2$(C_5R_5), (R = Ph, 5a; R = Me, 5b). The complexes **5a,b** were prepared in a one-step procedure involving the complexation of the butadiyne ligand of **3a,b** onto the $[(Cp^*)Fe(dppe)]^+$ fragment in the presence of KPF_6 to favor the iron-chlorine bond dissociation.[31,32] *In situ* deprotonation of the cationic intermediate, resulting in the complexation of the σ-metalated butadiyne at the Cp*Fe(dppe) unit, is subsequently achieved by addition of 1 equiv of a strong base.[6,29] Thus, treatment of $Fe(\eta^5\text{-}C_5Re_5)Fe(CO)_2$-$(C{\equiv}CC{\equiv}CH)$ (**3a,b**) KPF_6, and $KOBu^t$ in methanol with 1 equiv of Cp*Fe(dppe)Cl (**4**) produced a brown solution from which the binuclear μ-butadiynediyl complexes $(C_5Me_5)(dppe)Fe(C{\equiv}CC{\equiv}C)Fe(CO)_2(C_5R_5)$ (R = Ph, **5a**; R = Me, **5b**) were isolated in 59−69% yield (Scheme 2). Subsequent crystallization gave analytically pure **5a** and **5b**, which were characterized by IR, multinuclear NMR, and Mössbauer spectroscopy. Several synthetic routes to binuclear diynyl complexes have been reported. Except for the synthesis of the [Fe]−C_4−[Fe] and [Re]−C_4−[Re] symmetric compounds,[6,33] which were obtained upon oxidative coupling of the corresponding transition-metal ethynyl derivatives, all other C_4 complexes were obtained from preformed diynyl building blocks.[18,34−39] More recently, a procedure based

(29) Connelly, N. G.; Gamasa, M. P.; Gimeno, J.; Lapinte, C.; Lastra, E.; Maher, J. P.; Narvor, N. L.; Rieger, A. L.; Rieger, P. H. *J. Chem. Soc., Dalton Trans.* **1993**, 2575−2578.

(30) Roger, C.; Hamon, P.; Toupet, L.; Rabaâ, H.; Saillard., J.-Y.; Hamon, J.-R.; Lapinte, C. *Organometallics* **1991**, *10*, 1045−1054.

(31) Bruce, M. I.; Swincer, A. G. *Adv. Organomet. Chem.* **1987**, *52*, 3940.

(32) Bruce, M. I. *Chem. Rev.* **1991**, *91*, 197−257.

(33) Zhou, Y.; Seyler, J. W.; Weng, W.; Arif, A. M.; Gladysz, J. A. *J. Am. Chem. Soc.* **1993**, *115*, 8509−8510.

(34) Sonogashira, K.; Kataoka, S.; Takahashi, S.; Hagihara, N. *J. Organomet. Chem.* **1978**, *160*, 319−327.

(35) Fyfe, H. B.; Mlekuz, M.; Zargarian, D.; Taylor, N. J.; Marder, T. B. *J. Chem. Soc., Chem. Commun.* **1991**, 188−189.

(36) Stang, P. J.; Tykwinski, R. *J. Am. Chem. Soc.* **1992**, *114*, 4411−4412.

(37) Crescenzi, R.; Lo Sterzo, C. *Organometallics* **1992**, *11*, 4301−4305.

(38) Rappert, T.; Nürnberg, O.; Werner, H. *Organometallics* **1993**, *12*, 1359−1364.

(39) Bruce, M. I.; Hinterding, P.; Tiekink, E. R. T.; Skelton, B. W.; White, A. H. *J. Organomet. Chem.* **1993**, *450*, 209218.

Table 4. ^{57}Fe Mossbauer Fitting Parameters for Compounds 2−5

		δ, mm/s		ΔE_Q, mm/s		Γ, mm/s		% area	
compd	T (K)	Fe^{II}	Fe^{III}	Fe^{II}	Fe^{III}	Fe^{II}	Fe^{III}	Fe^{II}	Fe^{III}
2b	80	0.017		2.030		0.125		100	
2c	80	0.245		1.934		0.126		100	
2c	293	0.261		1.992		0.122		100	
3c	80	0.255		1.920		0.130		100	
5b	80	0.257		1.973		0.121		49.96	
		0.029		1.974		0.133		50.04	
5b	293	0.192		1.978		0.100		49.91	
		−0.033		1.958		0.160		50.09	
5a$^+$	80	−0.048	0.160	1.922	0.865	0.160	0.300	49.8	50.2
5b$^+$	80	−0.028	0.206	1.990	0.922	0.132	0.216	48.5	49.8
5b$^+$	293	−0.050	0.152	1.967	0.838	0.230	0.179	49.0	49.9

on CuI-catalyzed reactions in diethylamine was reported. This route allowed the preparation of homo- and heterobimetallic complexes with a C_4 bridge.[40] Starting from the preformed iron butadiynyl complexes **3a,b**, we found a smooth route to the homobinuclear derivatives **5a,b** which required neither metal catalyst assistance nor a very strong deprotonating agent such as butyllithium. The procedure has also been extended to the preparation of heterobinuclear $-C_x-$ complexes that contain both rhenium and iron end groups.[41]

A significant improvement of the synthesis of **5b** was found by starting from **2b** and following a one-pot procedure. The (trimethylsilyl)butadiynyl organoiron complex **2b** was solubilized in a THF/methanol mixture (50/50) before being refluxed in the presence of a small excess of anhydrous potassium fluoride. The resulting dark suspension was cooled to −50 °C, and 2.2 volumes of methanol, the organoiron complex **4**, KPF_6, and KO^t-Bu were added. After the mixture was stirred overnight and slowly warmed to room temperature, a brick red solution was obtained, from which **5b** was isolated (85% yield).

The IR spectra of the complexes **5a,b** display two strong ν_{CO} band stretchings and one $\nu_{C\equiv C}$ absorption. The substitution of the terminal H in complexes **3a,b** by the Cp*Fe(dppe) unit lowers the IR frequency of the carbonyl groups and reveals thereby the occurrence of electronic communication between the metal centers through the $-C_4-$ spacer. Considering that the chemical shift of the Cp* ligand in the butadiynyl complexes **3b,c** are observed at δ 1.34 and 1.44, respectively, the two Cp* resonances observed at δ 1.47 and 1.54 in the ^{1}H NMR spectrum of the complex **5b** were attributed to the methyl groups of the C_5 ring bound to the Cp*Fe(dppe) and Cp*Fe$(CO)_2$ building blocks, respectively. The carbon atoms of the linkage were named $C_{\alpha-\delta}$, starting from the more electron rich iron building block Cp*Fe(dppe), and the ^{13}C carbon resonances of the butadiynyl ligand were again assigned on the basis of the J_{CP} coupling constants, assuming that $^4J_{CP}$ is larger than $^3J_{CP}$ as seen for **3c** (*vide supra*). On this basis a more upfield resonance was attributed to the C_γ carbon atom C_γ (δ 107.7) than to C_β (δ 108.3) in complex **5a**. The C_β (δ 108.5) carbon of **5b** is also observed at upper field relative to C_α (δ 107.4). The difference between the chemical shift of the C_α and C_δ carbon atoms indicates that the C_4 linkage is polarized. The replacement of the phenyl groups of the pentaphenylcyclopentadienyl species by methyl substituents induces an upfield shift of the C_α carbon at the remote end of the bridge. Again, this shows that the electronic effects are transmitted from one metal center to the other through the carbon chain.

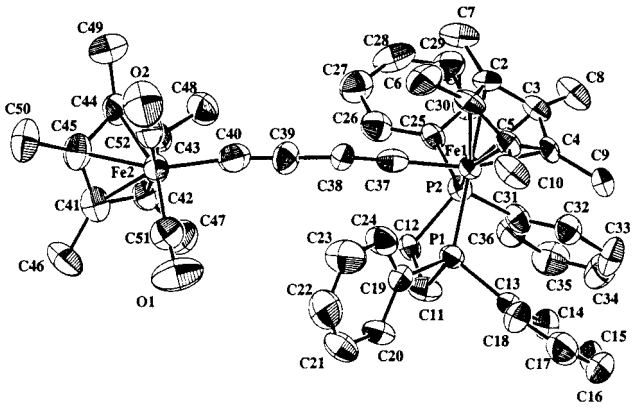

Figure 1. X-ray crystal structure of the complex (C_5Me_5)(dppe)Fe(C≡CC≡C)Fe$(CO)_2(C_5Me_5)$ (**5b**).

As already pointed out above, the isomeric shift of the Mössbauer doublet for the mononuclear complexes **2b,c** strongly depends on the nature of the ancillary ligand coordinated to the iron centers. Accordingly, the Mössbauer spectrum of the diiron compound **5b** recorded at zero field (80 K) displays two well-separated doublets with the same areas (Table 4). Both doublets have almost the same quadrupole splitting. This is characteristic of piano-stool iron(II) complexes with a very weak temperature dependence. Depending upon the electron density at the iron centers, the isomeric shifts of the two doublets are quite different (δ = 0.257/0.192 and 0.029/−0.033 mm s^{-1} at 80/293 K, respectively), in agreement with a strong polarization of this homobinuclear compound. The isomeric shifts at δ 0.257 and 0.029 are assignated to the iron centers of the Cp*Fe(dppe) and Cp*Fe$(CO)_2$ building blocks, respectively, on the basis of the isomeric shift determined for the mononuclear complexes **2b,c**. In contrast with the behavior of the mononuclear species, the isomeric shift of the binuclear complex **5b** is temperature dependent and the separation between the two doublets is almost constant.

Crystals of **5b** were grown by vapor diffusion of *n*-pentane in a toluene solution of the binuclear complex. The unit cell contains four molecules. The molecular structure of compound **5b** is shown in Figure 1, and the X-ray data conditions are summarized in Table 5. Selected bond distances and bond angles are collected in Table 6. Complex **5b** crystallizes in the monoclinic space group $P2_1/n$. The two metal centers clearly adopt a pseudooctahedral geometry, as generally observed for the piano-stool complexes, with the Cp* ring occupying

(40) Bruce, M. I.; Ke, M.; Low, P. J. *Chem. Commun.* **1996**, 2405−2406.

(41) Gladysz, J. A.; Lapinte, C.; Paul, F.; Meyer, W. E. Work in progress.

Table 5. Experimental Crystallographic Data for 5b

formula	$C_{52}H_{54}Fe_2P_2O_2$
fw	884.65
cryst syst	monoclinic
space group	$P2_1/c$
a, Å	21.099(5)
b, Å	13.868(4)
c, Å	15.924(9)
β, deg	104.60(3)
V, Å^3	4509(2)
Z	4
D_{calcd}, g/cm^3	1.303
F(000)	1856
μ(Mo Kα), cm^{-1}	7.504
T, K	294
cryst size, mm	0.12 × 0.12 × 0.28
max 2θ, deg	50
scan	$\omega/2\theta = 1$
t_{max}/measure, s	60
variance of standards	0.9%
range of hkl	−23 to +22; 0−15; 0−17
no. of rflns measd	6854
no. od rflns obsd ($I > \sigma(I)$)	3240 (1.5σ)
R_{int} (from merging equiv rflns)	0.027
R (isotropic)	0.11
difference Fourier	0.63−0.32
final R	0.073
R_w	0.064
$w = 1/\sigma(F_o)^2 = [\sigma^2(I) + (0.04F_o^2)^2]^{-1/2}$	
Sw	2.99
residual density (Δ/σ), e Å^{-3}	0.40, 0.05

Table 6. Selected Bond Distances (Å) and Angles (deg) for 5b

Fe(1)−P(1)	2.190(3)	Fe(1)−C(37)	1.886(9)
Fe(1)−P(2)	2.172(3)	Fe(2)−C(40)	1.90(1)
Fe(2)−C(51)	1.76(1)	C(37)−C(38)	1.21(1)
Fe(2)−C(52)	1.73(1)	C(38)−C(39)	1.36(1)
Fe(1)−Cp*(centroid 1)	1.740(3)	C(39)−C(40)	1.24(1)
Fe(2)−Cp*(centroid 2)	1.706(3)	C(1)−C(2)	1.38(2)

P(1)−Fe(1)−P(2)	85.7(1)	C(51)−Fe(2)−C(52)	95.3(5)
P(1)−Fe(1)−C(37)	83.8(3)	C(51)−Fe(2)−C(40)	87.3(5)
P(2)−Fe(1)−C(37)	83.4(3)	C(52)−Fe(2)−C(40)	90.4(5)
Fe(1)−C(37)−C(38)	177.8(8)	Fe(2)−C(40)−C(39)	172.0(1)
C(37)−C(38)−C(39)	175(1)	Fe(2)−C(51)−O(1)	176(1)
C(38)−C(39)−C(40)	178.4(9)	Fe(2)−C(52)−O(2)	178(1)

three coordination sites and the carbon of the −C_4− bridge and the phosphorus atoms of the dppe or the two carbons of the carbonyl ligands occupying the other three sites. The C(51)−Fe(2)−C(52) angle is significantly more opened than the P(1)−Fe(1)−P(2) angle. The bond lengths and angles for both organoiron building blocks compare well with the data determined for other mononuclear complexes in the FeCp*(dppe) or FeCp*$(CO)_2$ series.[21,42−45] The volumes occupied by the two organoiron units are quite different and the steric protections of the two iron centers are very different. The relative orientation of the two organometallic building blocks defined by the planes of the two Cp* rings gives an angle of 126.9(4)°.

The mixed-valence complex **5b** is, to our knowledge, the first example of a donor−acceptor [ML_n]−C≡CC≡C−[$ML'_{n'}$] to be structurally characterized. However, several solid-state structures of symmetric bimetallic compounds (M = Ru, Re, Rh) with a butadiynediyl linkage have been reported.[39,46,47] It has been shown that the C≡C carbon triple bonds range between 1.19 and 1.21 Å and the central carbon−carbon single bond between 1.37 and 1.39 Å. Concerning the [Fe]−C_4−[Fe] linkage of **5b**, the X-ray data reveal shorter Fe−C and C≡C bond lengths on the electron-rich side of the molecule than on the electron-poor moiety. This is in agreement with the polarization of the electron density from the donor $Fe(P)_2$ center to the acceptor $Fe(CO)_2$ group already suggested by ^{13}C NMR data. The comparison of the iron−carbon and carbon−carbon bond distances has to be made with caution in the limit of the accuracy of the X-ray data. However, the differences in the bonding patern along the [Fe]−C_4−[Fe] axis could also be the result of effective π* back-bonding on the $Fe(P)_2$ side of the complex, as previously suggested from the IR data (*vide supra*). Thus, the length of the C37−Fe1 bond (1.886(9) Å) seems to be shorter than the C(40)−Fe(2) bond distance (1.90(1) Å), in agreement with an increased bond order on the more electron rich metal side. Comparison of the bond angles also shows an increase of the linearity of the Fe−C_4−Fe axis on this side of the molecule. Curiously, the C(37)−C(38) triple bond length (1.21(1) Å) is very close to the carbon−carbon triple bond of the butadiyne (1.218(2) Å), whereas the C(39)−C(40) triple bond (1.24(1) Å) is significantly longer than the distance observed in the organic molecule.[48−50] The length of the C(38)−C(39) single bond (1.36(1) Å) is shorter than the C−C bond distance of the butadiyne (1.384(2) Å). A distance similar to those determined for the central C−C bond of **5b** was observed in the case of the mixed-valence complex [Cp*(dppe)Fe(C≡CC≡C)Fe(dppe)Cp*][PF_6] (**6**).[6] Discussion of the bond length in this system is not straightforward. One should not forget that retrodonation occurs in the empty π* orbital set of the whole butadiynediyl ligand, whereas the metal-dπ−butadiynediyl-π interactions are filled/filled type interactions.[27] Both types of interactions are possible in this donor−acceptor polarized [Fe]−C≡CC≡C−[Fe′] assembly. As a result, a strong electronic communication between the two organometallic fragments is believed to occur via the carbon bridge. In the complex **5b** the distance between the two nonequivalent iron atoms is 7.57 Å. Cyclic voltammogram measurements were performed to determine the mutual interaction between the metal centers over this distance.

3. Cyclic Voltammetry Analysis of the Binuclear Diiron μ-Butadiynediyl Complexes (C_5Me_5)(dppe)-Fe(C≡CC≡C)Fe$(CO)_2(C_5R_5)$ (R = Ph, 5a; R = Me, 5b). The initial scans in the CV of the butadiyne-bridged binuclear complexes **5a,b** from −0.8 to +1.4 V display two oxidation waves in dichloromethane, showing that, at the electrode surface (Figure 2), the neutral dimers undergo two successive one-electron oxidations to yield the mono- and dications, respectively. The data for peak potentials and current ratio compiled in Table 3 are quite similar for **5a** and **5b**. The ΔE_p values are

(42) Weyland, T.; Lapinte, C.; Frapper, G.; Calhorda, M. J.; Halet, J.-F.; Toupet, L. *Organometallics* **1997**, *16*, 2024−2031.
(43) Hamon, P.; Toupet, L.; Hamon, J.-R.; Lapinte, C. *J. Chem. Soc., Chem. Commun.* **1994**, 931−932.
(44) Mahias, V.; Cron, S.; Toupet, L.; Lapinte, C. *Organometallics* **1996**, *15*, 5399−5408.
(45) Goddard, R.; Howard, J.; Woodward, P. J. *J. Chem. Soc., Dalton Trans.* **1974**, 2025−2027.
(46) Yam, V. W.-W.; Lau, V. C.-Y.; Cheung, K.-K. *Organometallics* **1996**, *15*, 1740−1744.
(47) Gevert, O.; Wolf, J.; Werner, H. *Organometallics* **1996**, *15*, 2806−2809.
(48) Beer, M. *J. Chem. Phys.* **1956**, *25*, 745−750.
(49) Coles, B. F.; Hitchcock, B. P.; Watson, D. R. M. *J. Chem. Soc., Dalton Trans.* **1975**, 442−445.
(50) Rubin, Y.; Lin, S. S.; Knobler, C. B.; Anthony, J.; Boldi, A. M.; Diederich, F. *J. Am. Chem. Soc.* **1991**, *113*, 6943−6949.

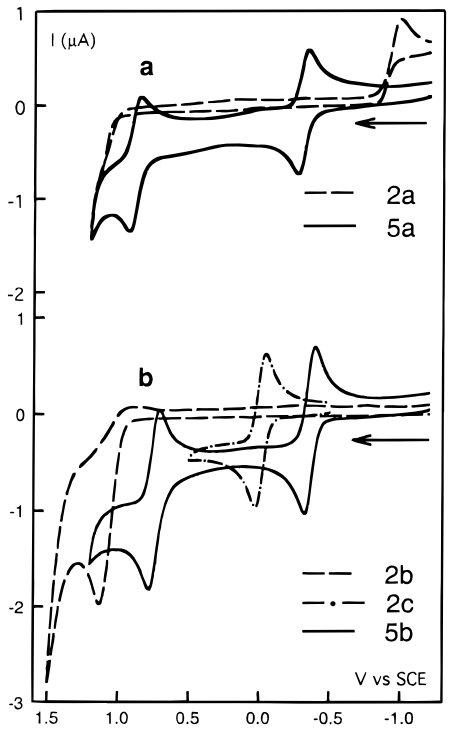

Figure 2. Cyclic voltammograms for $(C_5Me_5)(dppe)Fe(C{\equiv}CC{\equiv}C)Fe(CO)_2(C_5R_5)$ (a, R = Ph; b, R = Me) and related mononuclear complexes in 0.1 M $[nBu_4N][PF_6]/CH_2Cl_2$ (Pt electrode; V *vs* SCE; scan rate 0.100 V/s; 20 °C).

in the range 0.06−0.07 V, and the second redox process becomes reversible when the scan rate increases. For both compounds **5a** and **5b** the current ratio $i_p^c/i_p^a = 1$ for the first oxidation waves indicates the chemical reversibility of the first electron transfer and the thermal stability of the monocations **(5a,b)**$^+$. The i_p^c/i_p^a current ratio, less than unity, ranges from 0.8 to 0.9 (scan rate 0.1 V s^{-1}) for the second electron transfer, indicating that the dications **(5a,b)**$^{2+}$ slowly decompose at the platinum electrode. The comparison of the CV parameters with those of the corresponding monomers **2a**−**c** confirms the strong electronic communication between the metal centers across the all-carbon connector. Moreover, the role of the electron-donating−C_4−bridge is illustrated by comparison of the oxidation potential of the mononuclear electron-rich complex **2c**. The first oxidation potentials of the binuclear compounds **5a,b** are located at a potential 0.3 V less positive than for **2c**.

The quasi-reversibility of the second redox process is the result of the communication between the two iron building blocks across the connector but also constitutes a new illustration of the electron-donating role of the $-C_4-$ bridge. The comparison of the CV waves and the potential of the second almost-reversible redox process of **5a** and **5b** with the redox properties of **2a** and **2b** evidences a dramatic change (Figure 2). The increase of the reversibilty of the second oxidation process associated with an important diminution of the potential indicates a strong stabilization of the dioxidized species **[5a,b][PF$_6$]$_2$**. On the other hand, it is also noteworthy that the potentials measured for **5a** and **5b** are rather close (ΔE = 0.15 V), whereas it was shown that the replacement of the methyl substituents on the cyclopentadienyl ring by phenyl groups decreases the oxidation potential of mononuclear compounds by 0.5 V.[51] The original redox properties of these binuclear complexes

Scheme 3

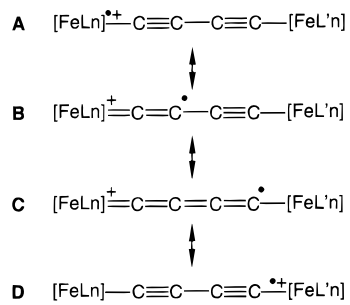

Scheme 4

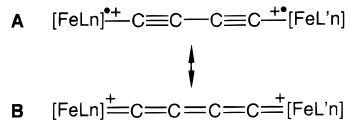

could be explained by the participation of the electron of the SOMO on the stabilization of both the mixed-valence species and the dications **[5a,b][PF$_6$]$_2$**. The delocalization of the odd electron on the metal center but also on the carbon atoms of the $-C_4-$ spacer could explain the diminution of the oxidation potential as well as the increased reversibility of the second oxidation process (Scheme 3). In fact, in the two oxidation processes, the electron should be removed from highly delocalized molecular orbitals all over the $L_nFe-C_4-FeL'_{n'}$ assembly and stabilized by participation of a cumulenic resonance structure depicted by the canonical form **B** in Scheme 4. However, despite a dramatic increase, the i^c/i^a current ratio is below unity for the second redox process and, as a consequence, the dications $[(C_5Me_5)(dppe)Fe(C{\equiv}CC{\equiv}C)Fe(CO)_2(C_5R_5)][PF_6]_2$ **(5a,b)**$^{2+}$ are not thermally stable enough to be considered as accessible synthetic targets.

4. Syntheses and Properties of the Mixed-Valence Complexes [(C$_5$Me$_5$)(dppe)Fe(C≡CC≡C)Fe(CO)$_2$(C$_5$R$_5$)][PF$_6$] (R = Ph, 5a[PF$_6$]; R = Me, 5b[PF$_6$]). On the basis of the CV results, oxidation **5** was carried out with $[Cp_2Fe][PF_6]$. The addition of 0.95 equiv of the oxidizing agent to **5** in CH_2Cl_2 resulted in a rapid color change from dark red to brown. After precipitation by pentane or diethyl ether, the Fe(III)−Fe(II) complexes **[5a,b][PF$_6$]** were isolated as deep green or dark brown powders in 85−90% yields (Scheme 2). Both salts are stable to heat and air for short periods of time, and their CV scans exhibit two waves identical with those of their Fe(II)−Fe(II) parents. These complexes were characterized by elemental analysis and Mössbauer, ESR, IR, UV−vis, and NIR spectroscopy.

It is well-documented that ^{57}Fe Mössbauer spectroscopy allows identification of the oxidation states of the iron centers.[52] The Mössbauer parameters of mononuclear and binuclear half-sandwich iron species are very different for Fe(II) and Fe(III).[6,30,52] The Mössbauer spectra of the complexes **5a,b** and **[5a,b][PF$_6$]** were run at 80 and 293 K, and the parameters (Table 4) show that the oxidation takes place on the Cp*Fe(dppe) side of the molecule. Expectedly, the spectra of the salts **[5a,b][PF$_6$]** clearly exhibit two doublets for localized Fe(II)−Fe(III) mixed-valence systems. From

(51) Brégaint, P.; Hamon, J.-R.; Lapinte, C. *J. Organomet. Chem.* **1990**, *398*, C25−C28.

(52) Greenwood, N. N. *Mössbauer Spectroscopy*; Chapman and Hall: London, 1971.

Table 7. ESR Data for [Cp*Fe(dppe)R]$^{\bullet+}$ in a $CH_2Cl_2/ClCH_2CH_2Cl$ (1/1) Glass at 77 K

compd	R	g_1	g_2	g_3
from ref 30	−H	1.9944	2.0430	2.4487
from ref 29	−C≡CH	1.987	2.034	2.457
2b$^+$	−C≡CC≡CSiMe$_3$	1.9719	2.0325	2.4857
5a$^+$	−C≡CC≡CFe(CO)$_2$(C$_5$Ph$_5$)	1.9867	2.0214	2.3474
5b$^+$	−C≡CC≡CFe(CO)$_2$(C$_5$Me$_5$)	1.9865[a]	2.0497	2.3343

[a] A_1 = 11.67 G.

the QS values it can be concluded that the electron vacancy is mainly localized on the Cp*Fe(dppe) organometallic fragment. Characteristic parameters of a 17-electron low-spin iron(III) metal center are observed, whereas the isomeric shift and quadrupole spliting of the $(C_5R_5)Fe(CO)_2$ moieties correspond to pure iron(II) centers. The very similar values observed for the IS and QS of the $(C_5Me_5)Fe(CO)_2$ unit in **2b**, **5b**, and **[5b][PF$_6$]** indicate that the electronic structure of this iron center is not very sensitive to the nature of the fragment σ-bound at the remote end of the $-C_4-$ linkage or, at least, that the Mössbauer spectroscopy is less suited than the IR spectroscopy to reveal these interactions (*vide infra*).

X-Band ESR spectra of the binuclear radical cations **[5a,b$^{\bullet+}$]** dissolved in a glass of $CH_2Cl_2/ClCH_2CH_2Cl$ (1/1) were run at 80 K. The ESR spectra exhibited three well-separated features corresponding to the three components of the **g** tensor (Table 7). In both spectra the resolution of the high-field component into a 1/2/1 triplet was observed, in agreement with a hyperfine coupling with two equivalent ^{31}P nuclei. The **g** tensors and ^{31}P couplings are very close to those previously observed for related iron(III) d^5 low-spin compounds. The large value usually observed for the g_3 tensor in this type of piano-stool iron(III) complexes was attributed to the energetic proximity of the singly occupied HOMO of predominant $d_{x^2-y^2}$ character with the doubly occupied levels.[30] However, it is noteworthy that the g_3 values observed for the binuclear one-electron radicals **5a**$^{\bullet+}$ and **5b**$^{\bullet+}$ are significantly weaker than those previously observed for the closely related mononuclear radical [Cp*Fe(dppe)(C≡CH)]$^{\bullet+}$ (Table 7).[29] The ESR spectrum of the butadiynyl iron radical [Cp*Fe(dppe)-(C≡CC≡CH)]$^{\bullet+}$ also exhibits a similar spectrum. The comparison of these values suggests that the HOMO in the binuclear species would be more separated from the levels of the SOMO orbitals. This could be the consequence of a repulsive interaction between the d orbitals of two metal centers across the carbon bridge, in agreement with the more negative oxidation potential.

The IR data in Table 1 show that the $-C\equiv C-$ bond stretching is observed in the Fe(II)−Fe(III) complex **[5b][PF$_6$]** at a significantly lower frequency than in the mononuclear species **5b**, indicating the σ-complexation of the two termini of the butadiynediyl bridge. In agreement with the Mössbauer and ESR data the canonical structure **A** (Scheme 3) mainly contributes to the description of the mixed-valence complexes **[5a,b][PF$_6$]**. Additionally, the IR data support a weak contribution of the resonance structures B and C. Comparisons of the ν_{CO} bond stretching of the binuclear neutral and monocationic complexes **5a,b** and **[5a,b][PF$_6$]** with those of the mononuclear species **2a,b** or **3a,b** provide the most direct indication of the opposite electronic effect of the Cp*Fe(dppe) and [Cp*Fe(dppe)]$^+$ organometallic building blocks. The 18-electron Cp*Fe(dppe) group is more electron donating than the hydrogen atom and produces a weak diminution of the carbonyl frequencies of the carbonyl ligands coordinated at the other iron center through the −C4− connector.

Table 8. Visible and Near-Infrared Spectral Data for the Mixed-Valence Complexes [5a,b][PF$_6$], [6][PF$_6$], and [7][PF$_6$]

compd	solvent	$1/D_{op} - 1/D_s$	λ_{max} (nm)	$10^{-3}\epsilon_{max}$ (M^{-1} cm^{-1})	ν_{max} (cm^{-1})
[5a][PF$_6$]	CH_2Cl_2	0.382	810	2.0	12 345
			a		
[5b][PF$_6$]	CH_2Cl_2	0.383	829	8.3	12 062
			1600	0.36	6 250
[5b][PF$_6$]	CH_3COCH_3	0.493	829		12 062
			1622	0.27	6 165
[5b][PF$_6$]	CH_3CN	0.526	829		12 062
			1609	0.27	6 215
[5b][PF$_6$]	MeOH	0.536	829		12 062
			1620	0.22	6 172
[6][PF$_6$]	CH_2Cl_2	0.382	575	17.39	17 391
			663	15.08	15 082
[7][PF$_6$]	CH_2Cl_2	0.382	619	4.80	16 155
			845	3.2	11 834
			1302	12	7 541
[7][PF$_6$]$_2$	CH_2Cl_2	0.382	619	7.87	16 155
			829	3.79	12 062

[a] Near-IR spectrum not recorded.

In contrast, the 17-electron radical cation [Cp*Fe(dppe)]$^+$ produces an increase of the carbonyl frequencies. This also supports a weak contribution of the resonance from D to the description of the electronic structure of the mixed-valence complex **[5a,b][PF$_6$]**. Consequently, the one-electron oxidation/reduction process might allow control of the molecular dipolar moment. Such a property is of interest for the design of electrochemically switchable NLO/active materials.

The visible spectroscopy of transition-metal complexes is generally discussed with the assumption that the various spectroscopic transitions are classified as metal centered (MC), ligand centered (LC), metal to ligand charge transfer (MLCT), or ligand to metal charge transfer (LMCT). It was recently pointed out that this description constitutes a simplified picture.[53] This is particularly true for the σ-butadiynediyl-bridged transition-metal complexes, for which there is a large orbital mixing. The LC and MLCT configurations could lie very close in energy, as in some cyclometalated complexes.[54,55] Thus, assignment of the transition in the UV−vis spectrum of the neutral complexes **5a,b** and of the corresponding mixed-valence binuclear cations **[5a,b][PF$_6$]** is not straightforward. A maximum is observed around 210 nm, at the edge of the solvent absorption and features a great deal of shoulders alongside that spread over the visible range. The energy of these $\pi-\pi^*$ ligand-centered transitions is difficult to evaluate with precision, since no clear maxima could be observed above 350 nm. No other maximum is observed for the neutral complexes. An intense absorption at the limit between the visible range and near-infrared range is present in the spectrum of the oxidized dimers (Table 8). A similar observation of an intense absorption in the 700−900 nm region was previously done for related

(53) Serroni, S.; Juris, A.; Campagna, S.; Venturi, M.; Denti, G.; Balzani, V. *J. Am. Chem. Soc.* **1994**, *116*, 9086−9091.
(54) Maestri, M.; Balzani, V.; Deuschel-Cornioley, C.; Von Zelewsky, A. *Adv. Photochem.* **1992**, *17*, 1.
(55) Schmid, B.; Garces, F. O.; Watts, R. J. *Inorg. Chem.* **1994**, *33*, 9−14.

iron(III) complexes. For instance, the visible spectrum of the mononuclear iron(III) derivative [Cp*Fe(dppe)-(C≡C−C_5H_4)][PF_6] **[6][PF$_6$]**[56] and of the binuclear compounds [Cp*(dppe)Fe−C≡CC≡C−Fe(dppe)Cp*][PF_6]$_n$ (n = 1, 2; **[7][PF$_6$]$_n$**) show an intense absorption in the visible range[57] (Table 8). Since these bands have not been observed in the spectrum of their iron(II) relatives, we have tentatively attributed them to a ligand to metal charge transfer. However, as far as the −C_4− carbon chain is concerned, the localized MO approach may no longer be valid and transitions between poorly localized orbitals can be involved.

The ICT character of the absortion at 829 nm was excluded by the observation of the electronic spectrum of the unstable dioxidized species **[5b][PF$_6$]$_2$**. The CV data indicated that the dioxidized complex decomposes at 20 °C in less than a few minutes; however, it could be generated *in situ*. Thus, the complex **[5b][PF$_6$]** was directly oxidized in the spectroscopic cell by addition of silver hexafluorophosphate to a CH_2Cl_2 solution. Spectroscopic monitoring of the solution allowed observation of a shift of the absorption band to higher frequencies (762 nm) followed by a rapid disappearance of the absorption due to decomposition of the dioxidized complex, in agreement with the CV data. This gives no information regarding the intensity of the real extinction coefficient of the band at 762 nm, since the decomposition of the dication is concomitant with its formation. However, the similarity between the absorption spectra of **[5b][PF$_6$]** and **[5b][PF$_6$]$_2$** is strongly indicative of the LMCT character of this transition.

Examination of the near-infrared domain with close scrutiny, using a concentrated solution (10^{-2} M) of the very soluble mixed-valence complex **[5b][PF$_6$]**, did allow detection of another absorption at 1600 nm. This very broad and weak band is absent both in the neutral compound **5b** and in the *in situ* generated derivative **[5b][PF$_6$]$_2$**. It was shown that pseudooctahedral 17e complexes of manganese or chromium sometimes display very low energy electronic absorptions in the near-infrared.[58] We confirmed that the mononuclear iron(III) 17e species **[6][PF$_6$]** did not display such an electronic transition in the near-IR region.[59] Consequently, we ascribed the observed band at 1600 nm to an intervalence charge transfer (ICT) in **[5b][PF$_6$]**. The ICT bands of mixed-valence compounds can furthermore allow the calculation of the electronic coupling parameter V_{ab}. This parameter represents the adiabaticity of the electron transfer between the two redox centers, or in other words, it can be seen as the mixing between the HOMO orbitals of the metal centers with the π-orbital of the carbon chain.[17,60,61] For the class II valence-trapped asymmetric compounds the electronic coupling is weak. It is accessible from the Hush formula (V_{ab} in cm^{-1}, eq 1), in which R_{ab} is the distance between the metal centers in Å, ϵ_{max} is the extinction coefficient,

$$V_{ab} = \frac{2.06 \times 10^{-2}}{R_{ab}} (\epsilon_{max} \nu_{max} \Delta\nu_{1/2})^{1/2} \qquad (1)$$

ν_{max} is the transition energy, and $\nu_{1/2}$ is the full width at half-maximum in cm^{-1}.

From the near-IR data, the electronic parameter was calculated to be V_{ab} = 0.021 eV. A much larger value was found for the symmetrical mixed-valence complex **[7][PF$_6$]** (V_{ab} = 0.47 eV),[6] showing that the overlap between the the electronic wave functions of the donor and acceptor groups decrease abruptly with the energy difference between the donor and acceptor centers. We established also that the position of the maximum of the ICT band was virtually independent of the solvent. For the mixed-valence compounds the independence of the energy of the ICT with the solvent is generally interpreted as an indication of a weak inner-sphere and outer-sphere reorganization energy associated with the intramolecular electron transfer.[62] Comparison of the geometry of the iron(II) center in complex **5b** with that of the iron(III) compound [Cp*Fe(dppe)(CH_2OCH_3)]-[PF_6][63] indicates that the reorganization of the coordination sphere of the Cp*Fe(dppe) backbone should be weak upon the one-electron-oxidation process. Moreover, the large protection of the Fe−C_4−Fe axis provided by the bulky ligands bound at the metal centers strongly contributes to minimize the reorganization of the solvent molecules during the intramolecular electron transfer.

In conclusion, the electrochemical and spectroscopic studies performed on the donor−acceptor homobinuclear system [Fe]−C_4−[Fe′]$^{n+}$ show that the properties of the iron units in the molecular assemblies are different from their properties in individual organoiron complexes. Clearly, contribution of the four-carbon spacer takes place in the properties of the dinuclear species. In our mind, the key role played by the all-carbon spacer is 2-fold. First, it provides rigidity to the molecular backbone, and second, it makes possible new properties that the individual components do not possess. These properties originate from the large degree of covalency of the metal−carbon bonds, which favors mixing of the orbitals of the carbon linkage with those of the transition metals. Finally, such molecules can be considered as interesting models of polarized molecular wires. More importantly, we have also stated that the initial polarization could be reversed upon oxidation, thereby opening the possibility of external control or switching of the polarity. We believe that this kind of system has a high potential for the elaboration of new electronic devices.

Experimental Section

General Data. Reagent grade tetrahydrofuran (THF), diethyl ether, and *n*-pentane were dried and distilled from sodium benzophenone ketyl prior to use. Pentamethylcyclopentadiene was prepared according to the published procedure,[64] and other chemicals were used as received. All the manipulations were carried out under an argon atmosphere using Schlenk techniques or in a Jacomex 532 drybox under nitrogen. The FTIR spectra were recorded using a Nicolet instrument (Model 205) and KBr windows. Routine NMR spectra were recorded using a Bruker AW 80 MHz spectrom-

(56) Weyland, T. Synthesis and Properties of Bi- and Trinuclear Organoiron Complexes Having Different Oxidation States. PhD Dissertation, University of Rennes 1, 1997; p 231.
(57) Weyland, T.; Lapinte, C. Unpublished results (see Table 8).
(58) Atwood, C. G.; Geiger, W. E. *J. Am. Chem. Soc.* **1994**, *116*, 10849−10850.
(59) Weyland, T.; Lapinte, C. Unpublished results.
(60) Hush, N. S. *Prog. Inorg. Chem.* **1967**, *8*, 391−444.
(61) Sauvage, J.-P.; Collin, J.-P.; Chambron, J.-C.; Guillerez, S.; Coudret, C. *Chem. Rev.* **1994**, *94*, 993−1019.
(62) Creutz, C.; Taube, H. *J. Am. Chem. Soc.* **1973**, *95*, 1086−1094.
(63) Roger, C.; Toupet, L.; Lapinte, C. *J. Chem. Soc., Chem. Commun.* **1988**, 713−714.
(64) Kohl, F. X.; Jutzi, P. *J. Organomet. Chem.* **1983**, *243*, C37−C38.

eter. High-field NMR experiments were performed on a multinuclear Bruker 300 MHz instrument (AM300WB). Chemical shifts are given in parts per million relative to tetramethylsilane (TMS) for ^{1}H and ^{13}C NMR spectra and H_3PO_4 for ^{31}P NMR spectra. Cyclic voltammograms were recorded using a PAR 263 instrument and a saturated calomel electrode. Potentials are given in volts vs SCE, and the ferrocene−ferrocenium couple was used as an internal calibrant for the potential measurements ($E_0 = 0.460$ V vs SCE).[65] X-Band ESR spectra were recorded on a Bruker ESP-300E spectrometer. Mössbauer spectra were recorded with a 2.5×10^{-2} Ci (9.25×10^8 Bq)^{57}Co source using a symmetric triangular sweep mode.[66] Elemental analyses were performed at the Center for Microanalyses of the CNRS at Lyon-Solaise, France.

Fe(η^5-C_5Ph_5)(CO)$_2$(C≡CC≡CSiMe$_3$) (2a). A 2.2 M commercial solution of MeLi·LiBr (0.855 mL, 1.88 mmol) in diethyl ether was syringed into a cooled solution (−80 °C) of Me$_3$SiC≡CC≡CSiMe$_3$ (0.365 g, 1.88 mmol) in 15 mL of THF with stirring. The translucent solution was slowly warmed to room temperature (20 °C). After approximately 4 h of total stirring, this solution was cooled and Fe(η^5-C_5Ph_5)(CO)$_2$Br (1.0 g, 1.57 mmol) in THF was subsequently added at −80 °C. Then the cold reaction medium was warmed to ambient temperature overnight and the solvent was removed *in vacuo*. The precipitate was extracted with a mixture of *n*-pentane and diethyl ether (50/50), and the extract was filtered on a degassed alumina plug before being concentrated to dryness. The remaining pale brown solid was washed with 10 mL of *n*-pentane and dried *in vacuo*, giving 0.800 g of **2a** (75%). Anal. Calcd for $C_{44}H_{34}FeO_2Si$: C, 77.87; H, 5.05. Found: C, 78.50; H, 4.89. FT-IR (KBr/Nujol, cm^{-1}): ν 1984, 2024 (s, CO); 2129, 2185 (s, C≡C). ^{1}H NMR (300 MHz, C_6D_6): δ_H 0.12 (s, 9H, Si(CH_3)$_3$); 6.5−7.5 (m, 25H, 5C$_6H_5$). ^{13}C NMR (75 MHz, C_6D_6): δ_C 212.8 (s, *C*O); 125−135 (m, 5*C*$_6$H$_5$); 104.0 (s, *C*$_5$Ph$_5$); 99.8 (s, *C*≡CC≡CSiMe$_3$); 99.4 (s, C≡*C*C≡CSiMe$_3$); 92.6 (s, C≡C*C*≡CSiMe$_3$); 71.1 (m, C≡CC≡*C*SiMe$_3$); 0.35 (q, $^1J_{CH} = 120$ Hz, Si(*C*H$_3$)$_3$).

Fe(η^5-C_5Me_5)(CO)$_2$(C≡CC≡CSiMe$_3$) (2b). To a 15 mL solution of LiC≡CC≡CSiMe$_3$ in THF, prepared as described above from 4.350 mL of MeLi·LiBr (9.55 mmol) and 1.600 g of Me$_3$SiC≡CC≡CSiMe$_3$ (8.24 mmol), was added 2.750 g of Fe(η^5-C_5Me_5)(CO)$_2$I (7.41 mmol) in 50 mL of THF at −80 °C with stirring. The reaction medium was slowly warmed to ambient temperature overnight. Then the solvent was evaporated and the remaining brown oil diluted with 70 mL of diethyl ether. The pale brown suspension, shielded from light (aluminum foil), was added to 70 mL of *n*-pentane and eluted quickly on a degassed alumina column (10 cm) preloaded with 100 mL of a mixture of *n*-pentane and diethyl ether (50/50). Concentration of this solution *in vacuo* yielded 2.306 g of crude yellow-brown **2b** (85% yield). Pure **2b** can be obtained after recrystallization of the crude compound from 10 mL of *n*-pentane at −80 °C as a yellow powder (∼70% total yield). The compound **2b** is air stable in the solid form for short periods of time. It is a light-sensitive compound, especially in solution. It should be stored in the dark under an inert atmosphere. Anal. Calcd for $C_{19}H_{24}FeO_2Si$: C, 61.96; H, 6.57. Found: C, 62.23; H, 6.57. FT-IR (KBr/CH_2Cl_2, cm^{-1}): ν 2171, 2119 (w, C≡C); 2032, 2016 (m, CO); 1977 (s, CO). ^{1}H NMR (300 MHz, C_6D_6): δ_H 1.28 (s, 15H, C_5Me_5), 0.18 (s, 9H, SiMe$_3$). ^{13}C NMR (75 MHz, C_6D_6): δ_C 214.3 (s, CO); 106.3 (s, *C*≡CC≡CSiMe$_3$); 97.4 (s, C_5Me_5); 96.5 (s, C≡*C*C≡CSiMe$_3$); 94.7 (s, C≡C*C*≡CSiMe$_3$); 69.5 (s, C≡CC≡*C*SiMe$_3$); 9.5 (q, $^1J_{CH} = 128$ Hz, C_5*Me*$_5$); 0.6 (q, $^1J_{CH} = 117$ Hz, SiMe$_3$).

Fe(η^5-C_5Me_5)(η^2-dppe)(C≡CC≡C-SiMe$_3$) (2c). Photolysis (with a Hanovia lamp equipped with a quartz jacket, 450 W, 250 nm) of Fe(η^5-C_5Me_5)(CO)$_2$(C≡CC≡C-SiMe$_3$) (0.800 g, 2.17 mmol) in a mixture of toluene and acetonitrile (95/5) in the presence of bis(diphenylphosphino)ethane (0.865 g, 2.17 mmol) over 4 h gave a red-orange solution. Removal of the solvents yielded a dark red solid that was washed twice with 2 mL of cold ether (−40 °C). The remaining red powder was identified as complex **2c** (1.100 g, 70%). Anal. Calcd for $C_{43}H_{48}FeP_2Si$: C, 72.67; H, 6.81. Found: C, 72.82; H, 7.24. FT-IR (KBr/Nujol, cm^{-1}): ν 2166 (w, C≡C); 2090 (s, CO); 1980 (m, CO). FTIR (KBr/CH_2Cl_2, cm^{-1}): ν 2162 (w, C≡C); 2081 (s, C≡C); 1977 (m, C≡C). ^{31}P NMR (121 MHz, C_6D_6): δ_P 99.6 (s). ^{1}H NMR (300 MHz, C_6D_6): δ_H 7.93−6.99 (m, 20H, Ph); 2.48, 1.69 (2m, 4H, PCH$_2$); 1.39 (s, 15H, C_5Me_5); 0.24 (s, 9H, SiMe$_3$). ^{13}C NMR (75 MHz, C_6D_6): δ_C 142.2 (t, $^2J_{PC} = 38$ Hz, *C*≡CC≡CSiMe$_3$); 139.2−126.3 (m, Ph); 102.3 (t, $^3J_{PC} = 2$ Hz, C≡*C*C≡CSiMe$_3$); 96.2 (t, $^4J_{PC} = 3$ Hz, C≡C*C*≡CSiMe$_3$); 89.1 (s, C_5Me_5); 64.7 (s, C≡CC≡*C*-SiMe$_3$); 33.1−28.9 (m, CH$_2$); 10.7 (q, $^1J_{CH} = 126$ Hz, C_5Me_5); 1.8 (q, $^1J_{CH} = 119$ Hz, SiMe$_3$).

Fe(η^5-C_5Ph_5)(CO)$_2$(C≡CC≡CH) (3a). Potassium fluoride (0.040 g, 0.73 mmol) was added to a solution of Fe(η^5-C_5Ph_5)(CO)$_2$(C≡CC≡CSiMe$_3$) (0.500 g, 0.73 mmol) in a 20 mL methanol/THF mixture (50/50). The solution was refluxed overnight. After removal of the solvents under vacuum, the residue was extracted with toluene. Solvent was then evaporated from the extract, and the remaining solid was washed twice with 10 mL of *n*-pentane before being dried *in vacuo* to yield 0.300 g of brown **3a** (85%). Anal. Calcd for $C_{41}H_{26}FeO_2$: C, 81.20; H, 4.32. Found: C, 81.10; H, 5.00. FT-IR (KBr/Nujol, cm^{-1}): ν 3301 (w, C≡CH); 2141 (w, C≡C); 2033, 1988 (s, CO). ^{1}H NMR (300 MHz, C_6D_6): δ_H 6.5−7.5 (m, 25H, 5C$_6H_5$); 1.25 (s, 1H, C≡CC≡C*H*). ^{13}C NMR (75 MHz, C_6D_6): δ_C 213.0 (s, *C*O); 125−135 (m, 5*C*$_6$H$_5$); 103.7 (s, *C*$_5$Ph$_5$); 99.7 (d, $^3J_{CH} = 5$ Hz, C≡*C*C≡CH); 94.1 (s, *C*≡CC≡CH); 72.8 (d, $^2J_{CH} = 51$ Hz, C≡C*C*≡CH); 55.9 (d, $^1J_{CH} = 259$ Hz, C≡CC≡*C*H).

Fe(η^5-C_5Me_5)(CO)$_2$(C≡CC≡CH) (3b). In a Schlenk tube wrapped with aluminum foil, Fe(η^5-C_5Me_5)(CO)$_2$(C≡CC≡CSiMe$_3$) (1.530 g, 4.18 mmol) was solubilized in a 60 mL THF/methanol mixture (50/50) and refluxed for 3.5 h in the presence of a slight excess of anhydrous potassium fluoride (0.279 g, 4.98 mmol). The brown solution was cooled to ambient temperature, extracted with four 50 mL portions of diethyl ether, and filtered. Subsequent evacuation of the solvent, washing with 10 mL of *n*-pentane at −80 °C, and drying *in vacuo* yielded 1.040 g of crude yellow-brown **3b** (85% yield). Pure **3b** could be obtained after recrystallization of the crude precipitate from hot diethyl ether at −80 °C as a bright yellow powder (∼50% yield). The compound is air stable only in the solid form and for short periods of time. It is also light sensitive, especially in solution. It should be stored in the dark in an inert atmosphere. Anal. Calcd for $C_{16}H_{16}FeO_2$: C, 64.89; H, 5.45. Found: C, 65.05; H, 5.56. FT-IR (KBr/CH_2Cl_2, cm^{-1}): ν 3303 (w, C≡CH); 2141 (m, C≡C); 2026, 1976 (s, C≡O). ^{1}H NMR (300 MHz, C_6D_6): δ_H 1,34 (s, 15H, C_5Me_5); 1.32 (s, 1H, C≡CC≡C*H*). ^{13}C NMR (75 MHz, C_6D_6): δ_C 214.3 (s, *C*O); 102.9 (s, *C*≡CC≡CH); 97.4 (s, *C*$_5$); 95.0 (d, $^3J_{CH} = 6$ Hz, C≡*C*C≡CH); 73.4 (d, $^2J_{CH} = 51$ Hz, C≡C*C*≡CH); 54.1 (d, $^1J_{CH} = 216$ Hz, C≡CC≡*C*H); 9.5 (q, $^1J_{CH} = 128$ Hz, C_5*Me*$_5$).

Fe (η^5-C_5Me_5)(η^2-dppe)(C≡CC≡CH) (3c). To a solution of Fe(η^5-C_5Me_5)(dppe)(C≡CC≡CSiMe$_3$) (0.900 g, 1.27 mmol) in THF (20 mL) was added 0.20 equiv of tetrabutylammonium fluoride (TBAF). The solution was stirred for 4 h at room temperature. The solvent was then removed under vacuum and the residue was extracted with a mixture of toluene and ether (20/80). After evaporation, the solid was washed twice with 2 mL of cold ether and dried *in vacuo* to give 0.770 g of the deep red complex **3c** (95%). Anal. Calcd for $C_{40}H_{40}FeP_2 \cdot {}^1/_2Et_2O$: C, 74.67; H, 6.71. Found: C, 74.25; H, 6.24. FT-IR (KBr/Nujol, cm^{-1}): ν 3297 (m, C≡CH); 2099 (s, C≡C),1958 (w, C≡C). IR (KBr/CH_2Cl_2, cm^{-1}): ν 3300 (m, C≡CH); 2095 (s, C≡C), 1955 (w, C≡C). ^{31}P NMR (121 MHz, C_6D_6): δ_P 99.5 (s). ^{1}H NMR (300 MHz, C_6D_6): δ_H 7.99−6.98 (m, 20H, *Ph*); 2.54, 1.74 (2m, 4H, C*H*$_2$); 1.44 (s, 15H, C_5*Me*$_5$); 1.39 (s, 1H, C≡CC≡C*H*). ^{13}C NMR (75 MHz, C_6D_6): δ_C 139.3−126.3 (m, Ph); 136.6 (t, $^2J_{PC} = 38$ Hz, *C*≡CC≡CH); 100.7 (d, $^3J_{CH} = 5$ Hz, C≡*C*C≡CH); 88.5 (s, C_5Me_5); 75.1 (dt, $^2J_{CH} = 50$

(65) Connelly, N. G.; Geiger, W. E. *Chem. Rev.* **1996**, *96*, 877−910.
(66) Varret, F.; Mariot, J.-P.; Hamon, J.-R.; Astruc *D. Hyperfine Interact.* **1988**, *39*, 67−75.

Hz, $^4J_{PC}$ = 3 Hz, C≡C*C*≡CH); 50.5 (d, $^1J_{CH}$ = 248 Hz, C≡CC≡*C*H); 33.0−28.9 (m, CH_2); 10.3 (q, $^1J_{CH}$ = 126 Hz, C_5Me_5).

{Fe(η^5-C_5Me_5)(η^2-dppe)}(μ_2-C≡CC≡C){Fe(η^5-C_5Ph_5)(CO)$_2$} (5a). Fe(η^5-C_5Me_5)(η^2-dppe)(Cl) (0.500 g, 0.78 mmol), Fe(η^5-C_5Ph_5)(CO)$_2$(C≡CC≡CH) (0.500 g, 0.78 mmol), ^{t}BuOK (0.100 g, 0.93 mmol), and KPF_6 (0.173 g, 0.93 mmol) were suspended in 10 mL of methanol and the solution was stirred for 12 h at 40 °C. After removal of the solvent, the residue was extracted with toluene and the extract concentrated *in vacuo*. Addition of *n*-pentane precipitated a solid. Double washing with 10 mL of *n*-pentane and drying under vacuum allowed the isolation of 0.400 g of pure gray-green **5a** (59%). Anal. Calcd for $C_{77}H_{64}Fe_2O_2P_2$: C, 77.39; H, 5.40. Found: C, 76.7; H, 5.6. FT-IR (KBr/Nujol, cm^{-1}): ν 2102 (s, C≡C); 2022, 1976 (s, CO). UV (CH_2Cl_2): λ_{max} (ϵ/10^3 dm^3 M^{-1} cm^{-1}) 543 nm (1.5). ^{31}P NMR (121 MHz, C_6D_6): δ_P 100.6 (s, dppe). ^{1}H NMR (300 MHz, C_6D_6): δ_H 6.5−7.5 (m, 25H, 5C$_6H_5$); 1.48 (s, 15H, C_5Me_5). ^{13}C{^{1}H} NMR (75 MHz, C_6D_6): δ_C 214.6 (s, *C*O); 125−135 (m, 5*C*$_6$H$_5$); 114.4 (t, $^2J_{CP}$ = 42 Hz, C_α≡CC≡C); 108.7 (t, $^3J_{CP}$ = 3 Hz, C$_\alpha$≡*C*C≡C); 108.3 (t, $^4J_{CP}$ = 2 Hz, C$_\alpha$≡C*C*≡C); 103.2 (s, C_5Ph_5); 88.0 (s, *C*$_5$Me$_5$); 86.9 (s, C$_\alpha$≡CC≡*C*); 28−34 (m, CH_2(dppe)); 10.5 (q, $^1J_{CH}$ = 126 Hz, *C*$_5$Me$_5$).

{Fe(η^5-C_5Me_5)(η^2-dppe)}(μ_2-C≡CC≡C){Fe(η^5-C_5Me_5)(CO)$_2$} (5b). Fe(η^5-C_5Me_5)(η^2-dppe)Cl (0.340 g, 0.54 mmol), Fe(η^5-C_5Me_5)(η^2-dppe)(C≡CC≡CH) (0.200 g, 0.54 mmol), and KPF_6 (0.110 g, 0.59 mmol) were suspended at −40 °C in 60 mL of a methanol/THF mixture (50/50). A slight excess of KO^{t}Bu (0.075 g, 0.66 mmol) was added to this cold solution under argon, and the reaction medium was warmed to room temperature with vigorous stirring over 12 h. The solvents were evacuated, and the brown precipitate was extracted with toluene. The extract was concentrated *in vacuo* to ∼10 mL, and a red-orange product was precipitated by addition of 90 mL of *n*-pentane. This suspension was decanted, washed twice with 20 mL of *n*-pentane at −80 °C, and dried under vacuum, yielding 0.597 g of red complex **5b** (69%). Anal. Calcd for $C_{52}H_{54}Fe_2O_2P_2$: C, 70.60; H, 6.15. Found: C, 70.69; H, 6.30. FT-IR (KBr/CH_2Cl_2, cm^{-1}): ν 2102 (vw, C≡C); 2015, 1962 (s, CO). ^{31}P NMR (121 MHz, C_6D_6): δ_P 100.6 (s, dppe). ^{1}H NMR (300 MHz, C_6D_6): δ_H 8.16−7.02 (m, 20H, *Ph*); 2.74, 1.74 (2m, 4H, C*H*$_2$(dppe)); 1.54 (s, 15H, {Fe(η^5-C$_5$*Me*$_5$)(CO)$_2$}); 1.48 (s, 15H, {Fe(η^5-C$_5$*Me*$_5$)(η^2-dppe)}). ^{13}C NMR (75 MHz, C_6D_6): δ_C 216.0 (s, *C*O); 140.4−126.2 (m, *Ph*); 108.5 (t, $^3J_{CP}$ = 2 Hz, C$_\alpha$≡*C*C≡C); 107.4 (t, $^2J_{CP}$ = 41 Hz, *C*$_\alpha$≡CC≡C); 102.4 (t, $^4J_{CP}$ = 3 Hz, C$_\alpha$≡C*C*≡C); 96.6 (s, {Fe(η^5-*C*$_5$Me$_5$)(CO)$_2$}); 87.8 (s, {Fe(η^5-*C*$_5$Me$_5$)(η^2-dppe)}); 68.3 (s, C$_\alpha$≡CC≡*C*); 33.3, 29.2 (m, C*H*$_2$); 10.5, 9.8 (2s, $^1J_{CH}$ = 126, 128 Hz, Cp*).

One-Pot Synthesis of 5b from 2b. In a Schlenk flask wrapped with aluminum foil Fe(η^5-C_5Me_5)(CO)$_2$(C≡CC≡CTMS) (0.360 g, 0.98 mmol) was solubilized in a 20 mL mixture of THF and methanol (50/50) and this solution refluxed for 4 h in the presence of 1.2 equiv of anhydrous potassium fluoride (0.070 g, 1.20 mmol). The heterogeneous dark mixture was cooled to −50 °C and Fe(η^5-C_5Me_5)(η^2-dppe)Cl (0.610 g, 0.99 mmol), KPF_6 (0.200, 1.08 mmol), and KO^{t}Bu (0.130 g, 1.16 mmol) were subsequently added under argon. The reaction medium was then warmed to room temperature with stirring over 12 h and the deep red precipitate that was formed in the medium was decanted. Drying *in vacuo* yielded 0.585 g of crude **5b** (∼70%). Purer **5b** can be obtained after recrystallization from a toluene/*n*-pentane mixture (0.440 g, 50%).

X-ray Crystallography of 5b. Crystals for **5b** were obtained by slow vapor diffusion of *n*-pentane in a toluene solution of the complex at 20 °C (4 weeks). Crystal data and details of measurements are reported hereafter. Diffraction data were collected at 294 K on a CAD4 Enraf-Nonius automated diffractometer with graphite-monochromated Mo Kα radiation. Crystal data collection and refinement parameters are given in Table 5. The cell constants and orientation matrix for data collection were obtained from a least-squares refinement using a set of 25 high-θ reflections. After Lorentz and polarization corrections the structure was solved with SIR-92, which revealed many non-hydrogen atoms of the structure. The remaining ones were found after several scale factor and difference Fourier calculations. After isotropic (R = 0.11) and then anisotropic refinement (R = 0.089), many hydrogen atoms were found by a difference Fourier calculation (between 0.63 and 0.32 e Å^{-3}), and the remaining ones were set in theoretical positions. The whole structure was refined by full-matrix least-squares techniques (use of F magnitude; x, y, z, β_{ij} for Fe, P, O, and C atoms and x, y, z fixed for H atoms; 524 variables and 3240 observations). Atomic scattering factors from ref 67 were used. The calculations were performed on a Silicon Graphics Indy computer with the MOLEN package (ENRAF-Nonius, 1990).[68]

[{Fe(η^5-C_5Me_5)(η^2-dppe)}(μ_2-C≡CC≡C){Fe(η^5-C_5Ph_5)(CO)$_2$}][PF$_6$] ([5a][PF$_6$]). [Fe(C_5H_5)$_2$][PF_6] (0.125 g, 0.92 equiv) was added to a solution of {Fe(dppe)(η^5-C_5Me_5)}(μ_2-C≡CC≡C){Fe(η^5-C_5Ph_5)(CO)$_2$} (0.500 g, 0.42 mmol) in 10 mL of dichloromethane at −80 °C. Stirring was continued for 2 h, while the reaction medium was warmed to room temperature. The solution was then concentrated, and **[5a][PF$_6$]** was precipitated as a deep green solid by addition of excess diethyl ether. After washing with ether and drying *in vacuo*, 0.480 g of pure product was obtained (86%). Anal. Calcd for $C_{77}H_{64}F_6Fe_2O_2P_3$: C, 69.02; H, 4.81. Found: C, 70.23; H, 4.67.

[{Fe(η^5-C_5Me_5)(η^2-dppe)}(μ_2-C≡CC≡C){Fe(η^5-C_5Me_5)(CO)$_2$}][PF$_6$] ([5b][PF$_6$]). [Fe(C_5H_5)$_2$][PF_6] (0.185 g, 0.92 equiv) was added to a solution of {Fe(η^5-C_5Me_5)(dppe)}(μ_2-C≡CC≡C){Fe(η^5-C_5Me_5)(CO)$_2$} (**5b**; 0.540 g, 0.62 mmol) in 10 mL of dichloromethane. Stirring was maintained 1 h at room temperature, and the solution was concentrated *in vacuo* to ∼2 mL. Addition of 50 mL of *n*-pentane allowed precipitation of a solid. Subsequent washing with four 5 mL portions of diethyl ether and drying under vacuum yielded 0.500 g of pure **[5b][PF$_6$]** as a dark brown product (89%). Anal. Calcd for $C_{52}H_{54}F_6Fe_2O_2P_3$: C, 60.66; H, 5.29. Found: C, 60.31; H, 5.38. IR (KBr/CH_2Cl_2, cm^{-1}): ν 2039, 1985 (m, CO); 1906 (s broad, C≡C).

Acknowledgment. We are grateful to Dr. A. Mari (Toulouse, France) for Mössbauer facilities and to Dr. J. Maher (Bristol, England) for ESR assistance.

Supporting Information Available: Complete tables of atomic coordinates and their estimated standard deviations, bond lengths and angles, and general temperature factor expressions for **5b[PF$_6$]** (12 pages). Ordering information is given on any current masthead page.

OM970730O

(67) *International Tables for X-ray Crystallography*; Kynoch Press (present distributor D. Reidel, Dordrecht, The Netherlands): Birmingham, U.K., 1974; Vol. IV.

(68) Enraf-Nonius Molecular Structure Determination Package; MolEN, version 1990; Enraf-Nonius, Delft, The Netherlands.